*Molecular Vision* 2019; 25:921-933 <http://www.molvis.org/molvis/v25/921>
Received 8 August 2019 | Accepted 30 December 2019 | Published 31 December 2019



# Functional characterization of a novel *GUCA1A* missense mutation (D144G) in autosomal dominant cone dystrophy: A novel pathogenic *GUCA1A* variant in COD

**Suzhen Tang,[1] Yujun Xia,[1] Yunhai Dai,[2] Yaning Liu,[1] Jingshuo Li,[1] Xiaojing Pan,[2] Peng Chen[1]**

**(The first two authors contributed equally to the manuscript.)**

*[1]Department of Human Anatomy, Histology and Embryology, School of Basic Medicine, Qingdao University, Qingdao266071, Shandong Province, China; [2]State Key Laboratory Cultivation Base, Shandong Provincial Key Laboratory of Ophthalmology, Shandong Eye Institute, Shandong First Medical University & Shandong Academy of Medical Sciences, Qingdao, China*

**Purpose:** To elucidate the clinical phenotypes and pathogenesis of a novel missense mutation in *guanylate cyclase activator A1A* (*GUCA1A*) associated with autosomal dominant cone dystrophy (adCOD).
**Methods:** The members of a family with adCOD were clinically evaluated. Relevant genes were captured before being sequenced with targeted next-generation sequencing and confirmed with Sanger sequencing. Sequence analysis was made of the conservativeness of mutant residues. An enzyme-linked immunosorbent assay (ELISA) was implemented to detect the cyclic guanosine monophosphate (cGMP) concentration. Then limited protein hydrolysis and an electrophoresis shift were used to assess possible changes in the structure. Coimmunoprecipitation was employed to analyze the interaction between GCAP1 and retGC1. Immunofluorescence staining was performed to observe the colocalization of GCAP1 and retGC1 in human embryonic kidney (HEK)-293 cells.
**Results:** A pathogenic mutation in *GUCA1A* (c.431A>G, p.D144G, exon 5) was revealed in four generations of a family with adCOD. *GUCA1A* encodes guanylate cyclase activating protein 1 (GCAP1). D144, located in the EF4 loop involving calcium binding, was highly conserved in the species. GCAP1-D144G was more susceptible to hydrolysis, and the mobility of the D144G band became slower in the presence of $Ca^{2+}$. At high $Ca^{2+}$ concentrations, GCAP1-D144G stimulated retGC1 in the HEK-293 membrane to significantly increase intracellular cGMP protein concentrations. Compared with wild-type (WT) GCAP1, GCAP1-D144G had an increased interaction with retGC1, as detected in the coimmunoprecipitation assay.
**Conclusions:** The newly discovered missense mutation in *GUCA1A* (p.D144G) might lead to an imbalance of $Ca^{2+}$ and cGMP homeostasis and eventually, cause a significant variation in adCOD.

Cone dystrophy (COD) and cone-rod dystrophy (CORD) are retinal diseases that can be inherited as dominant, recessive, or X-linked traits [1] but are mainly acquired through autosomal dominant (ad) inheritance. They are characterized by damage to vision, abnormal color vision, and varying degrees of nystagmus and photophobia in the early stage, followed by peripheral visual field loss and even blindness [1]. CORD involves progressive loss of cone photoreceptor function followed by gradual loss of rod cell function, and it is usually accompanied by retinal degeneration [1]. However, in hereditary progressive COD, only the cone function is impaired, with retinal degeneration limited to the central retina. Clinical phenotypes of COD have significant heterogeneity, so the performance of each patient in the same family can range from photoaversion to cone dystrophy.

Ten disease-causing genes (*AIPL1*-gene ID: 23746; OMIM: 604392; *CRX*-gene ID:1406; OMIM: 602225; *GUCA1A*-gene ID: 2978; OMIM: 600364; *GUCY2D*-gene ID: 3000; OMIM: 600179; *PITPNM3*-gene ID: 83394; OMIM: 608921; *PROM1*-gene ID: 8842; OMIM: 604365; *PRPH2*-gene ID: 83394; OMIM: 608921; *RIMS1*-gene ID: 22999; OMIM: 606629; *SEMA4A*-gene ID: 64218; OMIM: 607292, and *UNC119*-gene ID: 9094; OMIM: 604011) and four loci (*CORD4*-gene ID: 9094; OMIM: 604011;

*CORD12*-gene ID: 8842; OMIM: 604365; *CORD17*-gene ID: 101409267; OMIM: 615163, and *RCD1*-gene ID: 5953; OMIM: 180020) with unidentified genes have been found in adCOD and adCORD (RetNet). One of the most representative dominant CORD and COD genes is *guanylate cyclase activator A1A* (*GUCA1A*-gene ID: 2978; OMIM: 600364), encoding guanylate cyclase activating protein 1 (GCAP1) [2]. *GUCA1A* is located at 6p21.1 [3], and GCAP1 is expressed

Correspondence to: Peng Chen, Department of Human Anatomy, Histology and Embryology, School of Basic Medicine, Qingdao University, 308 Ningxia Road, Qingdao 266071, China; Phone: (532) 8378-0061; FAX: (532) 83780081; Email: chenpeng599205@126.com.

in the rods and cones as a member of the neuronal calcium sensor family of proteins [4]. This protein is essential for light transduction regulation and confers retinal photoreceptor cells with $Ca^{2+}$ sensitivity to retGC1 activity [5,6].

Mutations in *GCAP1* disrupt calcium binding in GCAP1 or affect GCAP1/retGC1 interaction [7], thus reducing the $Ca^{2+}$-dependent inhibition of GCAP1, and leading to increased retGC1 activity and levels of intracellular cyclic guanosine monophosphate (cGMP) [8,9]. Excessive levels of cGMP have been shown to cause retinal degeneration [10,11].

In recent years, 21 mutations in *GUCA1A* have been identified in patients with vision-threatening retinal diseases [10,12-18], including COD, CORD, macular dystrophy (MD), and central areolar choroidal dystrophy (CACD). Nine missense mutations in *GUCA1A* have been found in COD (Table 1). This study illustrates a novel missense mutation in *GUCA1A* (c.431A>G, p.D144G, exon 5) in four generations of a family with adCOD. With functional prediction and analysis, we identified the pathogenic effect of GCAP1-D144G, which can lead to increased retGC1 activity and result in persistently high levels of cGMP. This may also represent a possible mechanism for the formation of adCOD.

## METHODS

*Participants and clinical examination:* Four generations of a family with adCOD were recruited at theQingdao eye hospital of Shandong Eye Institute (Qingdao,China). There were 16 members in the family (7 affected, 9 unaffected; 7 males, 9 females). The 7 affected patients included (I:I, male, 82 years; II:2, female, 63 years; II:3, male, 61 years; III:2, female, 38 years;III:3, male, 37 years; IV:2, female, 8 years; IV:3, male, 15 years).The 9 unaffected patients included (I:2, male, 70years; II:1, male, 65 years; II:4, male, 61 years; III:1, male, 39 years; III:4, male, 37 years; III:5, male, 35 years; III:6, female, 33 years; IV:1, female, 10 years; IV:4, female, 9 years).They all had no other systemic abnormalities. Two hundred individuals with no medical history associated with any ophthalmic diseases were included in the control group. All participants received a comprehensive ophthalmic examination, including measurement of visual acuity and intraocular pressure, color vision testing, fundoscopy, multifocal electroretinography, and optical coherence tomography (OCT). The study was conducted according to the principles of the Declaration of Helsinki and was approved by the Ethics Committee of Qingdao University with informed consent from all participants. Written informed consent were obtained from all participants.

*Genetic testing:* Peripheral venous blood (5 ml) of the participating family members was sampled, and genomic DNA was extracted with a DNA isolation kit for mammalian blood (Tiangen, Beijing, China). Venous blood and genomic DNA samples were stored at −80 °C before use. The proband (III:2) underwent next-generation sequencing captured with 532 inherited genes related to the genetic visual system. The exon regions of these genes were particularly enriched with a biotinylated capture probe (Joy Orient Translational Medicine Research, Beijing, China). Burrows-Wheeler Aligner (BWA) software was used to perform short-read mapping and alignment, while SOAPsnp software and GATK Indel Genotype were used to test single nucleotide polymorphism (SNP) and insertion and deletion mutations, respectively. Identified mutants were filtered in databases. Sanger sequencing verified whether any remaining variants were cosegregated with the family disease phenotype. The novel mutations in *GUCA1A* were also genotyped with Sanger sequencing in the 200 normal control subjects. The possible pathogenicity of the mutations was predicted using the Sorting Intolerant from Tolerant (SIFT) algorithm, Polymorphism Phenotyping v2 (PolyPhen-2), Protein Variation Effect Analyzer (PROVEAN), and MutationTaster.

*Sequence alignment and structure modeling of GCAP1:* The human GCAP1 protein (NP_000400.2) sequence was aligned for analysis of the conservation of the mutated residues with the sequences of the following orthologous proteins: *Bos taurus* (NP_776971), *Danio rerio* (NP_571945), *Gallus gallus* (NP_989651), *Mus musculus* (NP_032215), *Rattus norvegicus* (NP_001100357), *Takifugu rubripes* (NP_001027790), and *Xenopus tropicalis* (NP_001096291). Multiple alignments were made using ClustalX2 software. The SWISS-MODEL was used to model the homology structure of the GCAP1 mutant based on the chicken wild-type (WT) GCAP1 (Protein Data Bank identifier: 2r2i), and three-dimensional (3D) models of proteins were constructed via PyMol software.

*Preparation of plasmids and cloning, protein expression, and purification:* Glutathione-S-transferase (GST)-tagged GCAP1 (GST-GCAP1) was generated via PCR amplification of human GCAP1 cDNA and inserted into pGEX-4T-1. After an initial denaturation step at 94 °C for 3 min, 35 PCRcycles (denaturation: 94 °C, 40 s; annealing: 52 °C, 40 s; extension: 72 °C, 2 min) and a final extension step at 72°C for 10 min were performed. For FLAG-tagging, full-length GCAP1 was inserted into pcDNA3.1. For green fluorescent protein (GFP)-tagging, full-length retGC1 was inserted into the pEGFP-N1 vector to obtain the recombinant plasmid pEGFP-retGC1. GCAP1-D144G was created with PCR amplification and confirmed with sequencing. The methods for expressing fusion proteins were the same as previously described [19].

**Table 1. List of known and novel mutations of *GUCA1A* gene.**

| Nucleotide change | protein change | Region | Type | PolyPhen2 | SIFT | PROVEAN | Mutation taster | Diagnosis |
|---|---|---|---|---|---|---|---|---|
| c.149C>T | p.Pro50Leu | EF1-EF2 link | Missense | BEN | DEL | DEL | DIS | COD, CORD |
| c.250C>T | p.Leu84Phe | EF2helix F | Missense | PRO | TOL | DEL | DIS | MD |
| c.256G>C | p.Gly86Arg | EF2-EF3 hinge | Missense | PRO | DEL | DEL | DIS | MD |
| c.265G>A | p.Glu89Lys | EF2-EF3 link | Missense | POS | DEL | DEL | DIS | COD |
| c.296A>G | p.Tyr99Cys | EF3 helix E | Missense | PRO | DEL | DEL | DIS | COD |
| c.299A>G | p.Asp100Gly | EF3 loop, $Ca^{2+}$binding | Missense | PRO | DEL | DEL | DIS | CORD, MD |
| c.300T>A | p.Asp100Glu | EF3 loop, $Ca^{2+}$binding | Missense | PRO | DEL | DEL | DIS | COD, CORD |
| c.302_304delTAG | p.Val101del | EF3 loop | Indel | N.A | N.A. | DEL | DIS | MD |
| c.304G>C | p.Asp102His | EF3 loop, $Ca^{2+}$binding | Missense | PRO | DEL | DEL | DIS | CORD |
| c.312C>A | p.Asn104Lys | EF3 loop, $Ca^{2+}$binding | Missense | PRO | DEL | DEL | DIS | COD |
| c.320T>C | p.Ile107Thr | EF3 loop | Missense | PRO | DEL | DEL | DIS | MD |
| c.332A>T | p.Glu111Val | EF3 loop, $Ca^{2+}$binding | Missense | BEN | DEL | DEL | DIS | CORD |
| c.341C>T | p.Thr114Ile | EF3 helix F | Missense | BEN | DEL | NEU | POL | P.U. |
| c.359–360delTT | p.Arg120Leu | EF3 loop, $Ca^{2+}$binding | Missense | N.A. | N.A. | NEU | DIS | CACD |
| c.428delTinsACAC | p.Ile143delinsAsnThr | EF4 helix E | Delins/Indel | N.A. | N.A. | DEL | POL | COD |
| c.431A>G | p.Asp144Gly | EF4 loop, $Ca^{2+}$binding | Missense | PRO | DEL | DEL | DIS | This study |
| c.444T>A | p.Asp148Glu | EF4 loop, $Ca^{2+}$binding | Missense | PRO | TOL | DEL | DIS | COD |
| c.451C>T | p.Leu151Phe | EF4 loop $Ca^{2+}$binding | Missense | PRO | DEL | DEL | DIS | COD, CORD |
| c.464A>G | p.Glu151Gly | EF4 loop, $Ca^{2+}$binding | Missense | PRO | DEL | DEL | DIS | COD |
| c.464A>C | p.Glu155Ala | EF4 loop, $Ca^{2+}$binding | Missense | PRO | DEL | DEL | DIS | COD |
| c.476G>T | p.Gly159Val | EF4 helix F | Missense | PRO | DEL | DEL | DIS | COD, CORD |
| c.526C>T | p.Leu176Phe | Carboxy terminal | Missense | PRO | TOL | NEU | DIS | MD |

EF, helix E-loop-helix F; $Ca^{2+}$-binding, $Ca^{2+}$-binding domain; PRO for probably damaging; POS for possibly damaging; BEN for benign; DEL for deleterious; TOL for tolerated; N.A. for not applicable; DEL for deleterious; NEU for neutral; DIS for disease causing; POL for polymorphism; P.U. for Pathogenetic unknow.

Fusion proteins GCAP1-WT and GCAP1-D144G were expressed from the PGEX-4T-1 vector in BL21 (DE3) competent *E. coli* cells. The overexpressed protein was subsequently purified as described previously [20] with some modifications. Cells was grown in standard Luria-Bertani (LB) medium (Solarbio, Beijing, China) containing 100 µg/ml ampicillin at 1.0 l, until they reached $A_{600}$ 0.6–0.7. After induction with 0.5 mM isopropyl β-D-thiogalactoside (IPTG) for 2 h, bacterial precipitation obtained with centrifugation at 956 ×g for 30 min at 4 °C was resuspended, and lysozyme was added into the buffer. The cells were then thawed and disrupted with ultrasonication, before 10 mg of streptomycin sulfate was added after the supernatant was centrifuged. The supernatant was centrifuged again, and 60 mg of glutathione agarose (Solarbio, Beijing, China) was added and incubated end-over-end for 2 h at 4 °C. The precipitate was washed with 30 ml of harvest buffer (1 M HEPES, 1 M NaCl, 1 mM benzamidine, and water) after 956 ×g centrifugation at 4 °C. The purity of the final purified GCAP1 protein determined with sodium dodecyl sulfate (SDS) gel electrophoresis was greater than or equal to 95%.

*Cell culture and transfection:* Human embryonic kidney (HEK)-293 cells (Appendix 1) were grown at 37 °C in 5% $CO_2$, incubated, and maintained in complete, high-glucose Dulbecco's modified Eagle's medium (HyClone, Logan, UT), which was supplemented with 10% fetal bovine serum and 1% penicillin-streptomycin. According to the manufacturer's instructions, the cells were transfected with Lipofectamine 2000 (Invitrogen, Carlsbad, CA). During the detection of protein stability, pcDNA3.1-GUCA1A-WT and pcDNA3.1-GUCA1A-D144G were transfected into the HEK-293 cells, and the protein supernatants were extracted for western blotting at 24, 48, and 72 h after transfection. To express retGC1 for the functional assay in vitro, the HEK-293 cells were transiently transfected with a 30 µg of pEGFP-retGC1 plasmid using Lipofectamine 2000 in a 90-mm culture dish according to the manufacturer's instructions.

*Coimmunoprecipitation and western blotting:* Coimmunoprecipitation (co-IP) and western blotting were performed as previously reported [19]. Briefly, HEK-293 cells were transfected with equal amounts of pcDNA3.1-GUCA1A-WT or pcDNA3.1-GUCA1A-D144G in the presence or absence of pEGFP-retGC1, followed by lysis in 1 ml of ice-cold lysis buffer containing 10 mM HEPES, 100 mM NaCl, 1 mM benzamidine, and 0.5% Triton X-100 (pH 7.4). After centrifugation, the lysates were incubated with anti-GFP antibody with protein-A/G agarose (Beyotime Biotechnology, Haimen, China) for 3 h. After being washed with cold wash buffer (10 mM HEPES, 100 mM NaCl, 0.1% Tween-20, benzamidine, and 3% bovine serum albumin [BSA]) three times, the immunoprecipitated proteins were eluted from the beads with SDS sample loading buffer. The co-IP assay was performed using anti-GFP affinity gel, while the bound proteins were detected with immunoblotting with anti-FLAG antibody. Then, the eluted samples were separated with SDS–polyacrylamide gel electrophoresis (PAGE), visualized with western blotting, and quantified by NIH Image 1.62. Each sample was normalized with glyceraldehyde-3-phosphate dehydrogenase (GAPDH). Primary antibodies included anti-FLAG antibody (Proteintech Group, Chicago, IL), anti-GFP antibody (Proteintech Group), and anti-GAPDH antibody (Kangchen, Shanghai, China).

*Limited protein hydrolysis of GCAP1:* Limited protein hydrolysis of purified GCAP1 and GCAP1-D144G was observed in SDS–PAGE in the presence or absence of 2.5 µM $Ca^{2+}$ as previously described [21]. Purified recombinant GCAP1 or GCAP1-D144G was incubated with trypsin at 30 °C, and the digest was analyzed with SDS-PAGE at 0, 5, 10, and 20 min.

*Immunofluorescence staining:* The HEK-293 cells were cotransfected with pEGFP-retGC1 and pcDNA3.1-GUCA1A-WT/D144G plasmid as previously reported. The following is a supplement to the protocol'sdetails. PEGFP-retGC1 and pcDNA3.1-GUCA1A-WT / D144G plasmids were co-transfected into HEK-293 cells with a GCAP1: retGC1 plasmid ratio of 1: 0.5. According to the reagent manufacturer's instructions, the cells were transfected with Lipofectamine 2000 The slides of the cells cultured in the standard glass coverslip chambers (four 2 $cm^2$ chambers per slide) were washed twice with PBS (1X; 8 mM $Na_2HPO_4$, 137 mM NaCl, 2mM $KH_2PO_4$, 2.6 mM, KCL, pH 7.2), fixed with 4% paraformaldehyde for 15 min, and washed again following permeation with 0.2% Triton X-100. After being blocked overnight with 5% normal goat serum, the samples were incubated with anti-FLAG antibody at 37 °C for 1 h, washed, and stained with a fluorescein-conjugated second antibody (donkey anti-rabbit immunoglobulin (IgG; $H^+L$; Life Technologies, Carlsbad, CA) at 37 °C for 30 min. The cell nucleus was counterstained with 4', 6-diamidino-2-phenylindole (DAPI) for 5 min and then washed as mentioned above. Cells were observed using a fluorescence microscope (CKX53, Olympus, Tokyo, Japan).

*ELISA:* pcDNA3.1-GUCA1A-WT and pcDNA3.1-GUCA1A-D144G were transfected into the HEK-293 cells. The cell pellets were divided into groups of EGTA (1 µM EGTA) and $Ca^{2+}$ (2.5 µM $Ca^{2+}$) after they were homogenized in 300 µl of lysis buffer with the added protease inhibitor cocktail.

Human retGC1 was expressed in the HEK-293 cells, and the washed cell membranes were prepared as previously

described [22]. Briefly, the membranes containing equal amounts of total protein were resuspended in GC buffer (100 mM KCl, 50 mM Mops, 7 mM 2-mercaptoethanol, 8 mM NaCl, 10 mM MgCl2, 1 mM EGTA). Cell membranes were incubated with equal amounts of purified GCAP1-WT/D144G proteins, and the cGMP concentrations were measured at different free $Ca^{2+}$ levels using a $Ca^{2+}$-EGTA buffer system (1 μM EGTA or 2.5 μM $Ca^{2+}$).

Protein concentrations were standardized by extracting the protein and using a bicinchoninic acid (BCA) protein assay kit. Human cGMP competition enzyme-linked immunosorbent assay (ELISA; human cGMP ELISA Kit; Mlbio, Shanghai, China) was used to determine the cGMP levels following the manufacturer's instructions.

*Statistical analysis:* SPSS 19.0 was used for statistical analysis, and quantitative data were analyzed by using the Student *t* test to compare groups. The data are presented as the mean ± standard deviation (SD), and a p value of less than 0.05 was considered statistically significant.

## RESULTS

*Clinical assessment and findings:* Ophthalmic examination confirmed that seven of 16 members across the four generations of the sampled family were affected by adCOD (Figure 1). All patients had similar features, including progressive vision loss, photophobia, nystagmus, color vision impairment, and visual field impairment. The proband (III:2) was a female patient aged 43 years at the time of observation. Her best corrected visual acuity was oculus dexter (OD) 0.1 and oculus sinister (OS) 0.05. The fundus appearance (Figure 2A,B) and macular OCT (Figure 2C) were consistent with the diagnosis. Patient IV:3 was first seen at age 16. His best corrected visual acuity was OD 0.5 and OS 0.4. His fundoscopy (Figure 3A,B) and macular OCT (Figure 3C) results were also in accordance with the diagnosis. For IV:3, the multifocal electroretinography examination showed that the amplitude density of the left eye's macular area was significantly reduced (Figure 3D). Humphrey visual field examination showed that the visual fields of both eyes were defected to different degrees (Figure 3E).

*Identification of GUCA1A as a candidate gene:* The proband (III:2) was genetically tested with exome sequencing of a set of candidate genes. The average sequence depth was 58.34, and 72.21% of the exon sequences were sequenced at least ten times. Sixty-two non-synonymous SNPs, two splicing sites, and one indel were selected according to the recommended filtering criteria. In exon 5 of *GUCA1A*, only a novel missense mutation (c.431A > G, p.D144G) was cosegregated in the family (Figure 4A and Table 1). This mutation was not found in the 200 control individuals. PolyPhen-2 and SIFT predicted that the D144G missense mutation would lead to harmful changes in the function of *GUCA1A* (Table 1).

D144 located in the EF4 hand loop was involved in calcium binding (Figure 4B,C). Multiple alignments of D144 of the GCAP1 protein from different species revealed 100% identification, which suggested it was highly conserved during evolution (Figure 4B). The homology structure of GCAP1-D144G (Figure 4C) showed that the hydrogen bonds between residue 144 and residue Phe140 or Gly147 in GCAP1 were eliminated due to substitution from Aspartyl (Asp) to Glycine (Gly) (Figure 4D).

*Regulation of retGC1 by GCAP1-WT and GCAP1-D144G:* We assayed the ability of GCAP1-WT and GCAP1-D144G to regulate retGC1in vitro (Figure 5A). The concentration of cGMP in the $Ca^{2+}$ group became lower than that in the EGTA group after induction by GCAP1-WT ($p<0.05$), whereas it was higher than that in the EGTA group due to induction by GCAP1-D144G ($p<0.01$). GCAP1-D144G caused a statistically significant increase in the cGMP concentration compared to GCAP1-WT ($p<0.01$) in the presence of $Ca^{2+}$. The same experimental result was also found in vitro (Figure 5B). GCAP1-D144G led to a higher increase of cGMP synthesis than did GCAP1-WT ($p<0.01$; Figure 5B).

*Biochemical analysis of GCAP1-D144G:* To detect the effect of GCAP1-D144G on the protein structure, limited protein hydrolysis experiments were performed. In the absence of $Ca^{2+}$, GCAP1-WT was readily susceptible to proteolysis after 5 min of exposure to trypsin, while GCAP1-D144G was completely digested (Figure 6A), indicating the open conformation of GCAP1-WT and D144G. Furthermore, the tight core of GCAP1-WT remained after 20 min of digestion in the

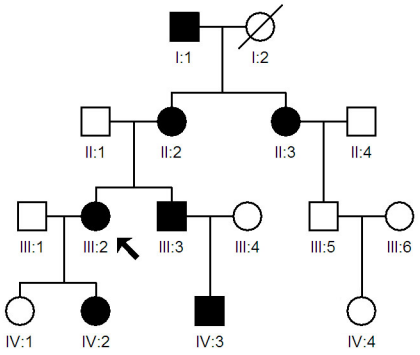


Figure 1. Pedigree of a Chinese family with COD. Squares and circles indicate males and females, respectively, and the filled symbols represent affected members. Deceased individuals are indicated with slashes (/). The arrow indicates the proband.

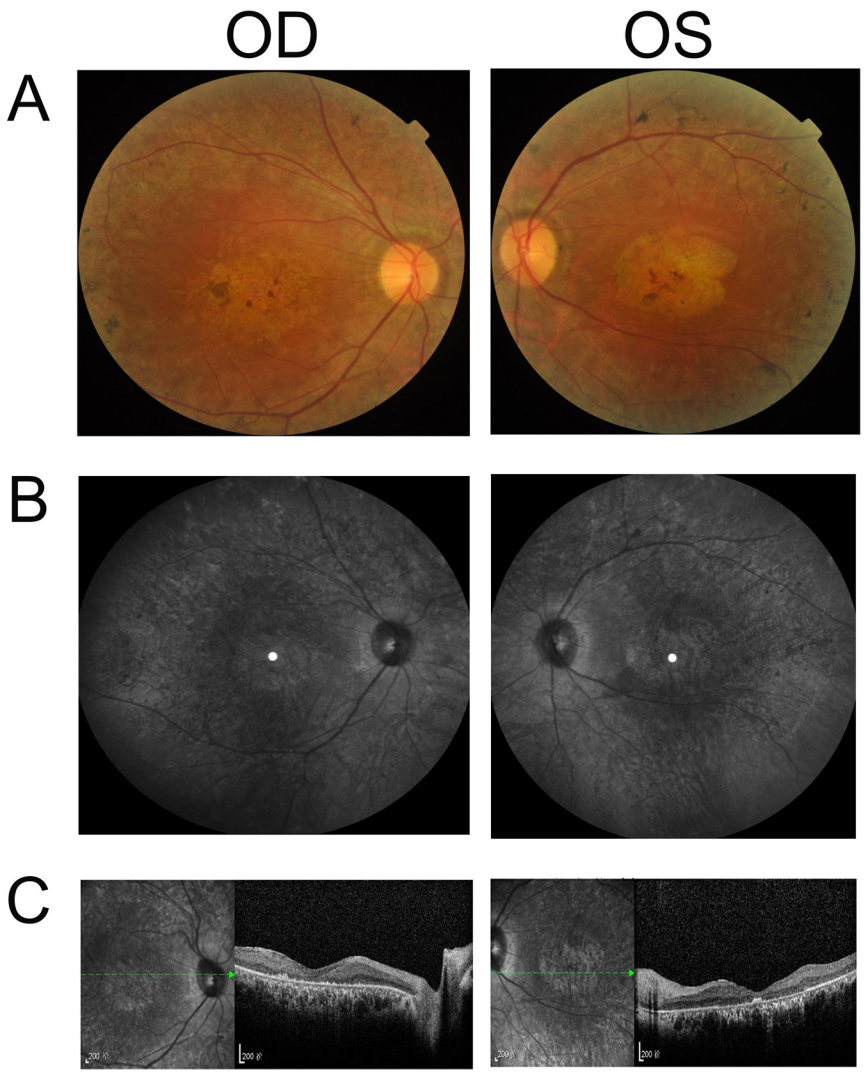


Figure 2. Phenotypic appearance of the COD proband (III:2). **A**: The fundus photograph shows that III:2 had oval lesions in the macular area and discoid depigmentation. The foveal reflex disappeared in both eyes. The macular area of her left eye is blue-gray with golden foil reflections, and the boundary is clear. There is irregular, patchy hyperplasia in her left eye. **B**: The infrared fundus photograph demonstrates the depigmentation zone in the macular area and slightly higher reflection in the mid-peripheral area. **C**: On the macular optical coherence tomography (OCT) images, the foveal centralis of both eyes is thin, and the ellipsoid and chimera bands are absent. Subepithelial hyper-reflexes are deposited, and choroidal capillary layer reflexes are enhanced in the foveal centralis. OD (right eye), OS (left eye).

presence of $Ca^{2+}$. Under the same condition, GCAP1-D144G was more susceptible to hydrolysis after 20 min of exposure to trypsin (Figure 6A). It indicated that GCAP1-WT exhibited a tighter conformation than D144G in the presence of $Ca^{2+}$.

The electrophoresis shift assay showed that GCAP1-WT exhibited a higher degree of electrophoretic mobility than GCAP1-D144G in the presence of $Ca^{2+}$ (Figure 6B), which was typical for calmodulin-like $Ca^{2+}$ binding proteins (the faster-moving, inactive form). However, the same experiment with GCAP1-D144G highlighted slower mobility during the electrophoresis shift assay in the presence of $Ca^{2+}$, indicating that the $Ca^{2+}$ induction of the mutant conformation was less pronounced, indicating a significantly decreased affinity for $Ca^{2+}$.

The expression levels and stability of GCAP1 in HEK-293 cells were analyzed with western blotting. With the extension of the transfection time, the GCAP1-WT protein levels remained almost unchanged (Figure 6C). However, the levels of GCAP1-D144G decreased statistically significantly in a time-dependent manner (Figure 6C). Even after 72 h of transfection, the expression levels of GCAP1-D144G were statistically significantly lower than those of GCAP1-WT ($p<0.01$; Figure 6C).

*Combination and colocalization of retGC1 and GCAP1-WT or GCAP1-D144G:* To determine whether GCAP1-WT/D144G was colocalized with retGC1, the HEK-293 cells were cotransfected with FLAG-GCAP1-WT/D144G and GFP-retGC1. GCAP1-WT and GCAP1-D144G exhibited a similar membrane distribution, predominantly endoplasmic

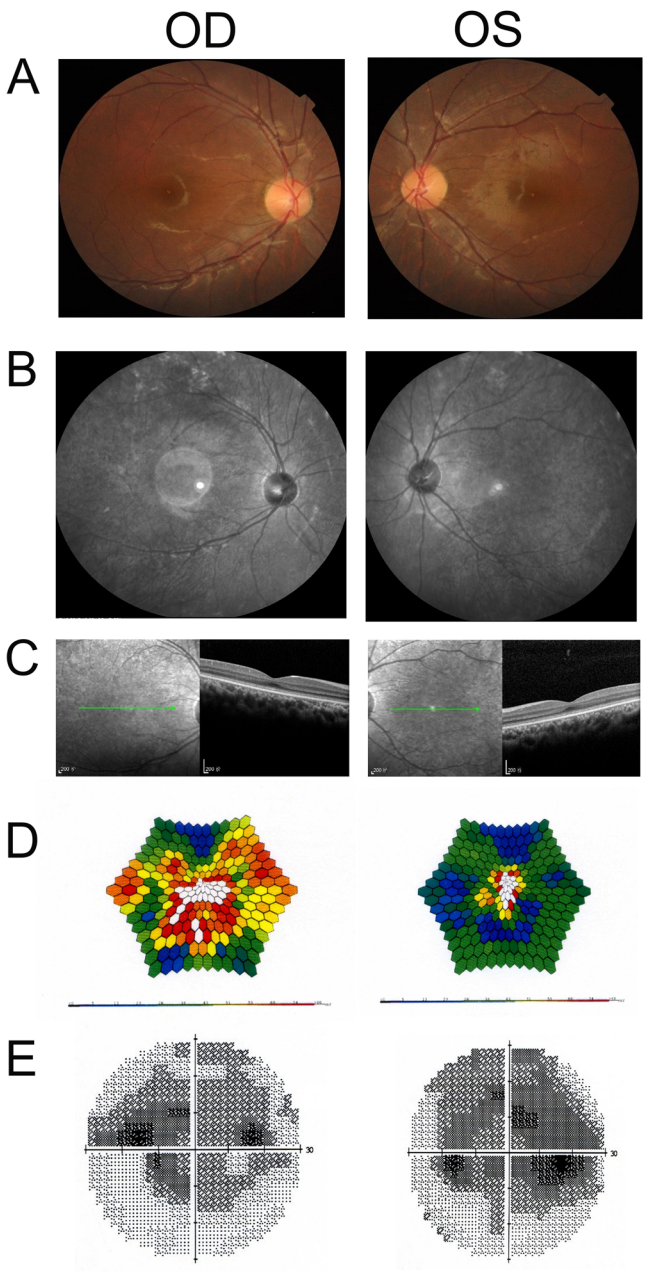


Figure 3. Phenotypic appearance of patient IV:3. **A**: Both eyes have a clear optic disc boundary and a slightly dark macular area. The left eye shows diffuse depigmentation (window-like defect) and generally normal retinal vessels, with no bleeding or exudation in the retina. **B**: A slightly high reflex zone is visible on the temporal lateral of the central macular fovea in the left eye on infrared fundus photography. **C**: The macular optical coherence tomography (OCT) examination shows that the band imaging of both eyes is slightly blurred. **D**: Multifocal electroretinography indicates that the amplitude density of the macular area in the left eye is significantly reduced. **E**: The Humphrey visual field examination disclosed that the visual field of both eyes has defects in different degrees.

reticulum membranes, when they were coexpressed with retGC1 (Figure 7A).

To test the ability of GCAP1-WT/D144G to bind to retGC1, co-IP experiments were performed. As shown in Figure 7B, the FLAG-GCAP1 protein was not detectable in the immunoprecipitated complex in the cells transfected with FLAG-GCAP1-WT or FLAG-GCAP1-D144G alone. In the cells cotransfected with FLAG-GCAP1 and GFP-retGC1, however, the FLAG-GCAP1 protein could be detected in its immunoprecipitated complex. GCAP1-D144G enhanced the association of GCAP1 with retGC1 in HEK-293 cells.

## DISCUSSION

Mutations in *GUCA1A* have been found in CORD, which is a blinding eye disease affecting 1/30,000 to 1/40,000 individuals [1]. Some common features of retinal dystrophies associated with these mutations have been identified [10,12-14]. However, the molecular characteristics do not necessarily relate to similar clinical phenotypes [10]. Therefore, the

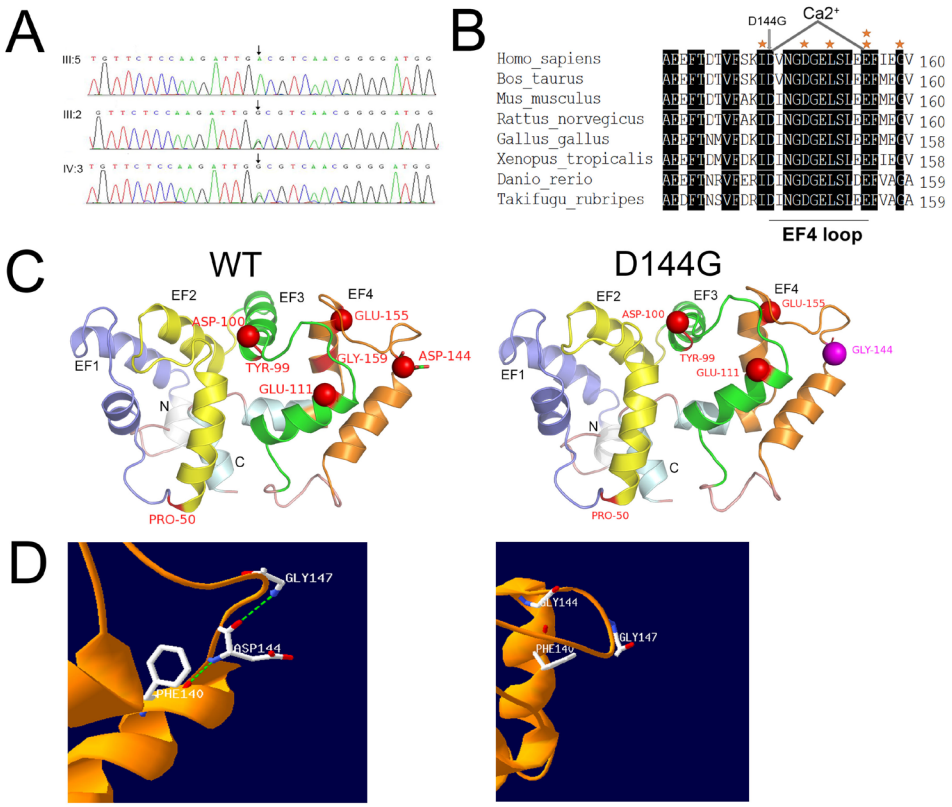


Figure 4. Location and structure of the D144G missense mutation. **A**: Sequence chromatograms of the detected mutations in *GUCA1A*. The top chromatogram represents the sequence of a healthy family member (III:5). The middle (III:2) and bottom (IV:3) chromatograms show a missense mutant sequence, which is A–G transversion in exon 5 of *GUCA1A*. The arrow indicates the location of the mutation. **B**: Orthologous protein sequence alignment of GCAP1 from multiple species. The 144 GLY of the EF4 loop region replaced the negatively charged ASP residue (arrows). Conservative residues are printed on a black background. The 12-amino-acid loop of the EF4-hand domains of the protein are underlined, and the other six known mutations are indicated with an asterisk. C: The structure of the GCAP1 three-dimensional homologous model. EF1 is slate, EF2 is yellow, EF3 is green, and EF4 is orange. The N- and C-terminal helixes are gray white and pale cyan, while the loop is deep pink. Mutated amino acids are indicated in red, and $Ca^{2+}$ ions are shown as red spheres. Residue D144 is shown as sticks, and 144 GLY is magenta and also shown as sticks. P50L is located in the EF1-EF2 link; Y99C, D100E, and E111V are located in EF3; and E155G, G159V, and D144G are located in EF4. **D**: Details of the region surrounding D144G. Hydrophobic residues showing persistent interactions with D144G are labeled as sticks. The hydrogen bonds are highlighted in green. The hydrogen bonds between residue 144 and residue Phe140 or Gly147 were eliminated upon changing from the wild-type ASP to mutant GLY.

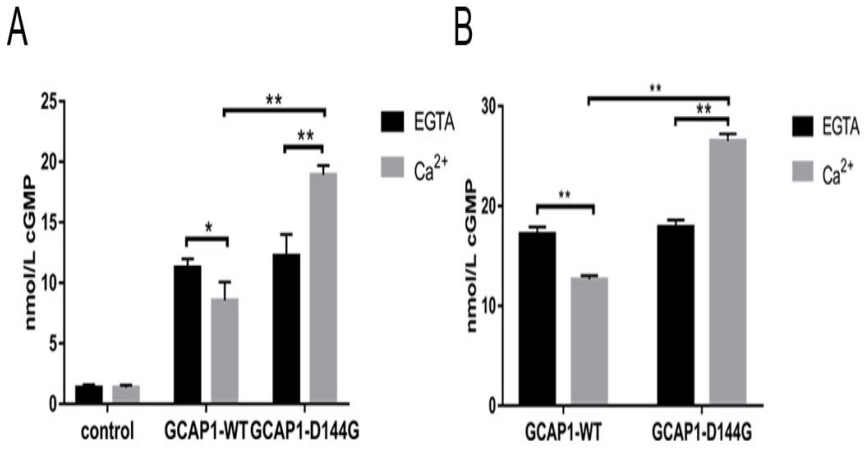


Figure 5. The levels of cGMP induced by retGC1 are regulated by GCAP1-WT/D144G in vitro. **A**: The levels of cyclic guanosine monophosphate (cGMP) induced by retGC1 in the human embryonic kidney (HEK)-293 cells are measured in the presence of GCAP1-WT/D144G. The free $Ca^{2+}$ concentration is 2.5 μM. The mock-transfected group was used as control. **B**: The levels of cGMP stimulated by transfected retGC1 in the HEK-293 cells were regulated by purification of GCAP1-WT/D144G. The free $Ca^{2+}$ concentration was 2.5 μM. The operation was repeated three times. Error bars were standard deviation.

molecular mechanism and function of each mutation must be investigated.

GCAP1 contains four EF hand motifs (EF1–4), with each containing a helix–loop–helix conformation [23]. EF1 and EF2 form the N-terminal domain, whereas EF3 and EF4 are contained in the C-terminal region [24]. EF1 is modified for the interface with guanylate cyclases (GCs) [25], while EF2, EF3, and EF4 bind to $Ca^{2+}$ [2]. Among the 21 previously reported mutations in *GUCA1A,* two were deletion mutations, and the others were missense mutations, including nine missense mutations found in patients with COD. This study recruited four generations of a family with adCOD exhibiting clinical phenotypes of adCOD, such as progressive vision loss, abnormalities of color vision, and nystagmus. Genetic tests detected a novel mutation in *GUCA1A* (c.431A>G,

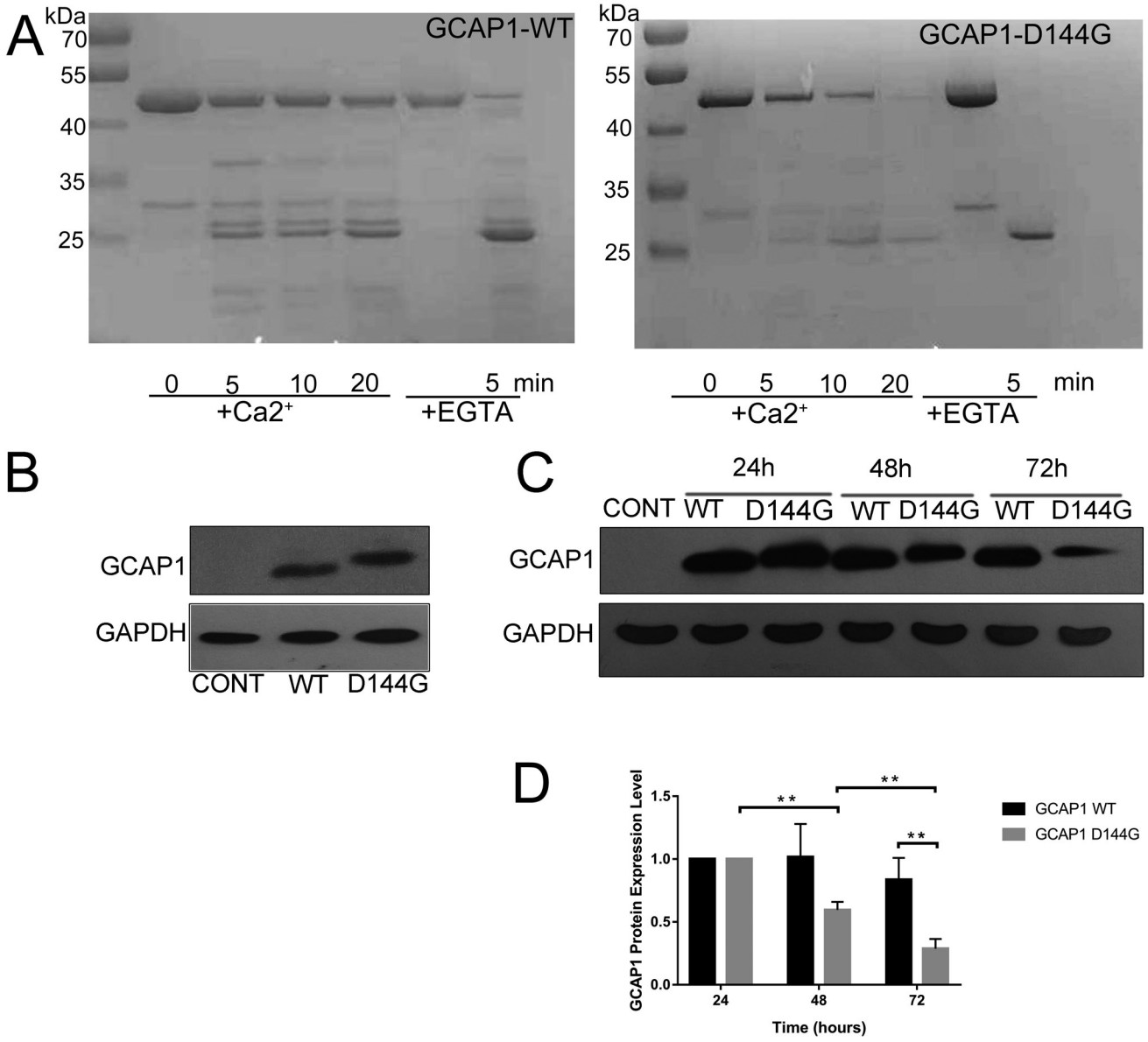


Figure 6. Biochemical analysis of GCAP1-D144G. **A**: Limited proteolysis of GCAP1-wild type (WT) and GCAP1-D144G by trypsin in the presence and absence of $Ca^{2+}$. Digestions were performed at 30 °C for 0, 5, 10, and 20 min. **B**: Electrophoresis shift assay of GCAP1-WT and GCAP1-D144G in the presence of 2.5 µM $Ca^{2+}$. **C**: The expression level and stability of GCAP1-WT and GCAP1-D144G in human embryonic kidney (HEK)-293 cells. GCAP1-WT and GCAP1-D144G were transfected into the HEK-293 cells. The proteins were detected using anti-FLAG antibody at 24, 48, and 72 h. The bars and error bars represent the mean ± standard deviation (SD) of three independent experiments, and the values within each experiment were normalized to those of glyceraldehyde-3-phosphate dehydrogenase (GAPDH). CONT, control.

p.D144G, exon 5) in the family. The characteristics of the clinical phenotypes, their molecular features, and specific functions of the mutant protein were subsequently evaluated.

Biochemically, most mutations in *GCAP1* are located in the EF hand regions. Ile143AsnThr [26], Leu151Phe [27-29], Glu155Gly [11], and Gly159Val [30], which are located in EF4, disrupt calcium binding in GCAP1 or affect GCAP1/retGC1 interactions [31]. Thus, reducing $Ca^{2+}$-dependent inhibition of GCAP1 could promote the constitutive activity of retGC1 and increase the intracellular cGMP levels [8,9,32], ultimately leading to photoreceptor death. The novel missense mutation (p.D144G) found in this research was also located in EF4. Biochemical results disclosed that the substitution of ASP with 144 GLY may partially impair GC1 inhibition, which constitutively activated retGC1 at the normal, dark $Ca^{2+}$ levels and generated a continuous increase in the intracellular cGMP levels. The calcium sensitivity effect of mutations in reducing GC stimulation has also been seen in Y99C [9], N104K [33], E111V [10], T114I [26], 143NT [26], L151F [27-29], and E155G [11].

Sequence analysis showed that the 144 ASP was highly conserved. It was necessary for the correct coordination of $Ca^{2+}$ in the EF4 loop with high affinity sites. The SWISS-MODEL was used to model the homology structure of GCAP1-D144G on the basis of GCAP1. It was shown that the hydrogen bonds between residue 144 and residue PHE140 or GLY147 in GCAP1-WT were eliminated due to the substitution of ASP with 144 GLY. These hydrogen bonds appeared to be important for the tertiary structure of the protein because they linked the EF3 helix and the EF4 loop. Therefore, GCAP1-D144G may result in the loss of hydrogen bonds in the protein, interfering with correct GCAP1 folding.

Limited protein hydrolysis experiments indicated that GCAP1-D144G was more susceptible to proteolysis. GCAP1-D144G cannot presume a compact $Ca^{2+}$-bound conformation, which was necessary for the inactivity in dark $Ca^{2+}$. The same effects have been observed in GCAP1-N104K [33], L151F [27,28], and I143NT [26]. GCAP1-N104K, located in the EF3 loop, was replaced by positive-charge amino acids and destroyed the binding of the EF3 hand to $Ca^{2+}$ [33]. GCAP1-L151F was in the β-folding of the EF4 hand, and its molecular dynamic confirmed that changes in the mutant structure affected the binding of $Ca^{2+}$ in the EF4 and EF2 hands [28]. GCAP1-I143NT was located on the EF4 hand helix. The substitution of Ile143 with two polar residues changed the

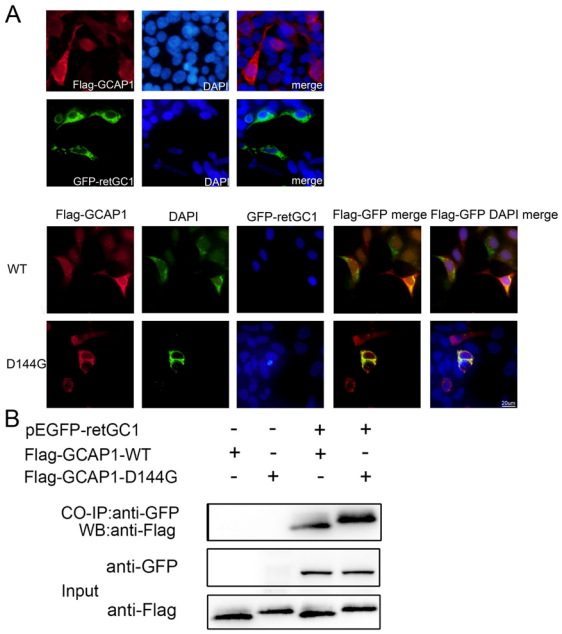


Figure 7. Cellular localization and combination of GCAP1 and retGC1. **A**: FLAG-GCAP1-wild type (WT)/D144G (red) and green fluorescent protein (GFP)-retGC1 (green) were coexpressed in human embryonic kidney (HEK)-293 cells. **B**: Interactions between FLAG-GCAP1-WT/D144G and GFP-retGC1 were detected with the co-IP assay. HEK-293 cells were cotransfected with FLAG-tagged GCAP1-WT or FLAG-GCAP1-D144G in the presence or absence of GFP-tagged retGC1. **A**: The precipitated complexes were probed with the FLAG antibody to detect FLAG-GCAP1-WT/D144G. The cell lysates were probed with the anti-GFP antibody and anti-FLAG antibody in western blotting for analysis of GFP-retGC1 expression (**B**) and FLAG-GCAP1-WT/D144G (**C**), respectively. WB, western blotting. IP, immunoprecipitation. The data are representative of three independent experiments.

orientation of the N-terminal α-helix, which reduced the affinity of the EF hands to $Ca^{2+}$ [26].

An electrophoretic shift assay showed that $Ca^{2+}$ binding resulted in lower electrophoretic mobility of GCAP1-D144G in the presence of 2.5 μM $Ca^{2+}$ while GCAP1-WT showed higher mobility. This suggested that the affinity of the mutant for $Ca^{2+}$ was significantly reduced. With respect to the protein stability, the expression levels of GCAP1-D144G significantly decreased as the transfection time was prolonged. The expression levels of the WT protein were almost identical, indicating a decrease in the stability of the mutant protein. Similarly, GCAP1-P50L showed decreased thermal stability [34]. These biochemical results illustrated that the *GCAP1*-D144G mutation could prevent proteins from folding into compact structures.

GCAP1 and retGC1 may control the recovery of light response in the photoreceptors of vertebrates through their molecular interactions and retGC1 in rods involved in regulating cGMP synthesis by negative calcium feedback [35]. Studies have shown that mutations in *GCAP1* or *retGC1* could alter the $Ca^{2+}$ sensitivity of cGMP synthesis or affect the GCAP1/retGC1 interaction [7,8,22,30,36,37]. Therefore, even at higher calcium concentrations, mutations in *GCAP1* can stimulate retGC1 [38], and ultimately, lead to degeneration and death of photoreceptors [10,11,13]. However, the mechanism by which mutations affect the GCAP1/retGC1 interaction is complex and difficult to understand [35]. GCAP1 activation of retGC1 may be performed either by direct binding or by indirect interaction [39]. Indirect interaction is consistent with the experimental results of previous studies on the binding of $Ca^{2+}$- and $Mg^{2+}$-saturated forms of retGC1 [40-42]. The conversion from activator to inhibitor status by $Ca^{2+}$ bound to EF4 in GCAP1 is a major determinant [43].

It was found that GCAP1-D144G not only displayed colocalization with retGC1 in the HEK-293 cells (Figure 7A) but also combined more retGC1 in the HEK-293 cells (Figure 7B). However, mutations in different parts of *GCAP1* disrupted the colocalization of GCAP1/retGC1, allowing most of the GCAP1 fluorescence to be evenly distributed across the cytoplasm and nucleoplasm [39]. We observed only the changes in colocalization caused by the mutation. The specific mechanism must be further explored. In addition, metal ligand binding in EF4 has been reported to have no significant effect on GCAP1 association with the cyclase [44]. The areas of GCAP controlling its ability to activate retGC1 are the interface between EF1, EF2, EF3, and the adjacent C-terminal region of EF4 [45,46]. EF1 has evolved in GCAPs to become the main part of the target-binding interface [39,40]. Moreover, EF2 and EF3 can be connected to retGC1 through the combination of $Ca^{2+}$ or $Mg^{2+}$ [44]. Therefore, it is suspected that the binding of GCAP1-D144G to retGC1 may strongly affect the indirect interaction or that the structure of EF1 can be remotely affected by $Ca^{2+}$ binding on the EF4 hand.

The process and mechanism of the interaction between GCAP1 and retGC1 after point mutation, as well as the changes in key residues and conformations involved, require further investigation. Based on the genetic testing and functional analyses, we concluded that the novel GCAP1-D144G mutation affected $Ca^{2+}$ sensitivity and the constitutive activation of retGC1 at high $Ca^{2+}$ levels, resulting in increased intracellular cGMP concentrations, and ultimately, likely adCOD. These findings help to introduce the diversity of phenotypes, providing guidance for clinical assessment and treatment of adCOD.

## APPENDIX 1. STR ANALYSIS.

To access the data, click or select the words "Appendix 1."

## ACKNOWLEDGMENTS

The authors thank all patients and their family for participating in the study. This work was supported by the National Natural Science Foundation of China (No. 81,970,782, No. 81,600,721), Shandong Provincial Natural Science Foundation (No. ZR2018MH016), Qingdao Postdoctoral Application Research Project (No. 40,518,060,071), China Postdoctoral Science Foundation (No. 2017M612211), Medical and Health Technology Development Project of Shandong Province (No. 2016WS0265), and Higher Educational Science and Technology Program of Shandong Province (No. J17KA235).
Dr. Peng Chen (chenpeng599205@126.com) and Dr. Xiaojing Pan (panxjcrystal@163.com) are co-corresponding authors for this study.

## REFERENCES

1. Hamel CP. Cone rod dystrophies. Orphanet J Rare Dis 2007; 2:7-[PMID: 17270046].

2. Baehr W, Palczewski K. Focus on molecules: guanylate cyclase-activating proteins (GCAPs). Exp Eye Res 2009; 89:2-3. [PMID: 19162008].

3. Subbaraya I, Ruiz CC, Helekar BS, Zhao X, Gorczyca WA, Pettenati MJ, Rao PN, Palczewski K, Baehr W. Molecular characterization of human and mouse photoreceptor guanylate cyclase-activating protein (GCAP) and chromosomal localization of the human gene. J Biol Chem 1994; 269:31080-9. [PMID: 7983048].

4. Burgoyne RD. Neuronal calcium sensor proteins: generating diversity in neuronal Ca2+ signalling. Nat Rev Neurosci 2007; 8:182-93. [PMID: 17311005].

5. Gorczyca WA, Polans AS, Surgucheva IG, Subbaraya I, Baehr W, Palczewski K. Guanylyl cyclase activating protein. A calcium-sensitive regulator of phototransduction. J Biol Chem 1995; 270:22029-36. [PMID: 7665624].

6. Dizhoor AM, Lowe DG, Olshevskaya EV, Laura RP, Hurley JB. The human photoreceptor membrane guanylyl cyclase, RetGC, is present in outer segments and is regulated by calcium and a soluble activator. Neuron 1994; 12:1345-52. [PMID: 7912093].

7. Behnen P, Dell'Orco D, Koch KW. Involvement of the calcium sensor GCAP1 in hereditary cone dystrophies. Biol Chem 2010; 391:631-7. [PMID: 20370318].

8. Sokal I, Li N, Surgucheva I, Warren MJ, Payne AM, Bhattacharya SS, Baehr W, Palczewski K. GCAP1 (Y99C) mutant is constitutively active in autosomal dominant cone dystrophy. Mol Cell 1998; 2:129-33. [PMID: 9702199].

9. Dizhoor AM, Boikov SG, Olshevskaya EV. Constitutive activation of photoreceptor guanylate cyclase by Y99C mutant of GCAP-1. Possible role in causing human autosomal dominant cone degeneration. J Biol Chem 1998; 273:17311-4. [PMID: 9651312].

10. Marino V, Dal Cortivo G, Oppici E, Maltese PE, D'Esposito F, Manara E, Ziccardi L, Falsini B, Magli A, Bertelli M, Dell'Orco D. A novel p.(Glu111Val) missense mutation in GUCA1A associated with cone-rod dystrophy leads to impaired calcium sensing and perturbed second messenger homeostasis in photoreceptors. Hum Mol Genet 2018; 27:4204-17. [PMID: 30184081].

11. Wilkie SE, Li Y, Deery EC, Newbold RJ, Garibaldi D, Bateman JB, Zhang H, Lin W, Zack DJ, Bhattacharya SS, Warren MJ, Hunt DM, Zhang K. Identification and functional consequences of a new mutation (E155G) in the gene for GCAP1 that causes autosomal dominant cone dystrophy. Am J Hum Genet 2001; 69:471-80. [PMID: 11484154].

12. Manes G, Mamouni S, Herald E, Richard AC, Senechal A, Aouad K, Bocquet B, Meunier I, Hamel CP. Cone dystrophy or macular dystrophy associated with novel autosomal dominant GUCA1A mutations. Mol Vis 2017; 23:198-209. [PMID: 28442884].

13. Peshenko IV, Cideciyan AV, Sumaroka A, Olshevskaya EV, Scholten A, Abbas S, Koch KW, Jacobson SG, Dizhoor AM. A G86R mutation in the calcium-sensor protein GCAP1 alters regulation of retinal guanylyl cyclase and causes dominant cone-rod degeneration. J Biol Chem 2019; 294:3476-88. [PMID: 30622141].

14. Chen X, Sheng X, Zhuang W, Sun X, Liu G, Shi X, Huang G, Mei Y, Li Y, Pan X, Liu Y, Li Z, Zhao Q, Yan B, Zhao C. GUCA1A mutation causes maculopathy in a five-generation family with a wide spectrum of severity. Genet Med 2017; 19:945-54. [PMID: 28125083].

15. Marino V, Scholten A, Koch KW, Dell'Orco D. Two retinal dystrophy-associated missense mutations in GUCA1A with distinct molecular properties result in a similar aberrant regulation of the retinal guanylate cyclase. Hum Mol Genet 2015; 24:6653-66. [PMID: 26358777].

16. Nong E, Lee W, Merriam JE, Allikmets R, Tsang SH. Disease progression in autosomal dominant cone-rod dystrophy caused by a novel mutation (D100G) in the GUCA1A gene. Doc Ophthalmol 2014; 128:59-67. [PMID: 24352742].

17. Huang L, Xiao X, Li S, Jia X, Wang P, Sun W, Xu Y, Xin W, Guo X, Zhang Q. Molecular genetics of cone-rod dystrophy in Chinese patients: New data from 61 probands and mutation overview of 163 probands. Exp Eye Res 2016; 146:252-8. [PMID: 26992781].

18. Huang L, Li S, Xiao X, Jia X, Sun W, Gao Y, Li L, Wang P, Guo X, Zhang Q. Novel GUCA1A mutation identified in a Chinese family with cone-rod dystrophy. Neurosci Lett 2013; 541:179-83. [PMID: 23428504].

19. Yang L, Wang Y, Chen P, Hu J, Xiong Y, Feng D, Liu H, Zhang H, Yang H, He J. Na(+)/H(+) exchanger regulatory factor 1 (NHERF1) is required for the estradiol-dependent increase of phosphatase and tensin homolog (PTEN) protein expression. Endocrinology 2011; 152:4537-49. [PMID: 21990315].

20. Peshenko IV, Dizhoor AM. Ca2+ and Mg2+ binding properties of GCAP-1. Evidence that Mg2+-bound form is the physiological activator of photoreceptor guanylyl cyclase. J Biol Chem 2006; 281:23830-41. [PMID: 16793776].

21. Rudnicka-Nawrot M, Surgucheva I, Hulmes JD, Haeseleer F, Sokal I, Crabb JW, Baehr W, Palczewski K. Changes in biological activity and folding of guanylate cyclase-activating protein 1 as a function of calcium. Biochemistry 1998; 37:248-57. [PMID: 9425045].

22. Tucker CL, Woodcock SC, Kelsell RE, Ramamurthy V, Hunt DM, Hurley JB. Biochemical analysis of a dimerization domain mutation in RetGC-1 associated with dominant cone-rod dystrophy. Proc Natl Acad Sci USA 1999; 96:9039-44. [PMID: 10430891].

23. Stephen R, Bereta G, Golczak M, Palczewski K, Sousa MC. Stabilizing function for myristoyl group revealed by the crystal structure of a neuronal calcium sensor, guanylate cyclase-activating protein 1. Structure 2007; 15:1392-402. .

24. Stephen R, Palczewski K, Sousa MC. The crystal structure of GCAP3 suggests molecular mechanism of GCAP-linked cone dystrophies. J Mol Biol 2006; 359:266-75. [PMID: 16626734].

25. Jiang L, Baehr W. GCAP1 mutations associated with autosomal dominant cone dystrophy. Adv Exp Med Biol 2010; 664:273-82. [PMID: 20238026].

26. Nishiguchi KM, Sokal I, Yang L, Roychowdhury N, Palczewski K, Berson EL, Dryja TP, Baehr W. A novel mutation (I143NT) in guanylate cyclase-activating protein 1 (GCAP1) associated with autosomal dominant cone degeneration. Invest Ophthalmol Vis Sci 2004; 45:3863-70. [PMID: 15505030].

27. Jiang L, Li TZ, Boye SE, Hauswirth WW, Frederick JM, Baehr W. RNAi-mediated gene suppression in a GCAP1(L151F)

cone-rod dystrophy mouse model. PLoS One 2013; 8:e57676-[PMID: 23472098].

28. Sokal I, Dupps WJ, Grassi MA, Brown J Jr, Affatigato LM, Roychowdhury N, Yang L, Filipek S, Palczewski K, Stone EM, Baehr W. A novel GCAP1 missense mutation (L151F) in a large family with autosomal dominant cone-rod dystrophy (adCORD). Invest Ophthalmol Vis Sci 2005; 46:1124-32. [PMID: 15790869].

29. Dell'Orco D, Behnen P, Linse S, Koch KW. Calcium binding, structural stability and guanylate cyclase activation in GCAP1 variants associated with human cone dystrophy. Cell Mol Life Sci 2010; 67:973-84. [PMID: 20213926].

30. Kitiratschky VB, Behnen P, Kellner U, Heckenlively JR, Zrenner E, Jagle H, Kohl S, Wissinger B, Koch KW. Mutations in the GUCA1A gene involved in hereditary cone dystrophies impair calcium-mediated regulation of guanylate cyclase. Hum Mutat 2009; 30:E782-96. [PMID: 19459154].

31. Vinberg F, Chen J, Kefalov VJ. Regulation of calcium homeostasis in the outer segments of rod and cone photoreceptors. Prog Retin Eye Res 2018; 67:87-101. [PMID: 29883715].

32. Vocke F, Weisschuh N, Marino V, Malfatti S, Jacobson SG, Reiff CM, Dell'Orco D, Koch KW. Dysfunction of cGMP signalling in photoreceptors by a macular dystrophy-related mutation in the calcium sensor GCAP1. Hum Mol Genet 2017; 26:133-44. [PMID: 28025326].

33. Jiang L, Wheaton D, Bereta G, Zhang K, Palczewski K, Birch DG, Baehr W. A novel GCAP1(N104K) mutation in EF-hand 3 (EF3) linked to autosomal dominant cone dystrophy. Vision Res 2008; 48:2425-32. [PMID: 18706439].

34. Newbold RJ, Deery EC, Walker CE, Wilkie SE, Srinivasan N, Hunt DM, Bhattacharya SS, Warren MJ. The destabilization of human GCAP1 by a proline to leucine mutation might cause cone-rod dystrophy. Hum Mol Genet 2001; 10:47-54. [PMID: 11136713].

35. Peshenko IV, Olshevskaya EV, Dizhoor AM. Evaluating the role of retinal membrane guanylyl cyclase 1 (RetGC1) domains in binding guanylyl cyclase-activating proteins (GCAPs). J Biol Chem 2015; 290:6913-24. [PMID: 25616661].

36. Olshevskaya EV, Ermilov AN, Dizhoor AM. Factors that affect regulation of cGMP synthesis in vertebrate photoreceptors and their genetic link to human retinal degeneration. Mol Cell Biochem 2002; 230:139-47. [PMID: 11952089].

37. Ramamurthy V, Tucker C, Wilkie SE, Daggett V, Hunt DM, Hurley JB. Interactions within the coiled-coil domain of RetGC-1 guanylyl cyclase are optimized for regulation rather than for high affinity. J Biol Chem 2001; 276:26218-29. [PMID: 11306565].

38. Sato S, Peshenko IV, Olshevskaya EV, Kefalov VJ, Dizhoor AM. GUCY2D Cone-Rod Dystrophy-6 Is a "Phototransduction Disease" Triggered by Abnormal Calcium Feedback on Retinal Membrane Guanylyl Cyclase 1. J Neurosci 2018; 38:2990-3000. [PMID: 29440533].

39. Peshenko IV, Olshevskaya EV, Lim S, Ames JB, Dizhoor AM. Identification of target binding site in photoreceptor guanylyl cyclase-activating protein 1 (GCAP1). J Biol Chem 2014; 289:10140-54. [PMID: 24567338].

40. Laura RP, Hurley JB. The kinase homology domain of retinal guanylyl cyclases 1 and 2 specifies the affinity and cooperativity of interaction with guanylyl cyclase activating protein-2. Biochemistry 1998; 37:11264-71. [PMID: 9698373].

41. Peshenko IV, Dizhoor AM. Activation and inhibition of photoreceptor guanylyl cyclase by guanylyl cyclase activating protein 1 (GCAP-1): the functional role of Mg2+/Ca2+ exchange in EF-hand domains. J Biol Chem 2007; 282:21645-52. [PMID: 17545152].

42. Koch KW, Dell'orco D. A calcium-relay mechanism in vertebrate phototransduction. ACS Chem Neurosci 2013; 4:909-17. [PMID: 23472635].

43. Lim S, Peshenko IV, Dizhoor AM, Ames JB. Structural insights for activation of retinal guanylate cyclase by GCAP1. PLoS One 2013; 8:e81822-[PMID: 24236217].

44. Peshenko IV, Olshevskaya EV, Dizhoor AM. Binding of guanylyl cyclase activating protein 1 (GCAP1) to retinal guanylyl cyclase (RetGC1). The role of individual EF-hands. J Biol Chem 2008; 283:21747-57. [PMID: 18541533].

45. Krylov DM, Niemi GA, Dizhoor AM, Hurley JB. Mapping sites in guanylyl cyclase activating protein-1 required for regulation of photoreceptor membrane guanylyl cyclases. J Biol Chem 1999; 274:10833-9. [PMID: 10196159].

46. Ermilov AN, Olshevskaya EV, Dizhoor AM. Instead of binding calcium, one of the EF-hand structures in guanylyl cyclase activating protein-2 is required for targeting photoreceptor guanylyl cyclase. J Biol Chem 2001; 276:48143-8. [PMID: 11584009].

Articles are provided courtesy of Emory University and the Zhongshan Ophthalmic Center, Sun Yat-sen University, P.R. China. The print version of this article was created on 31 December 2019. This reflects all typographical corrections and errata to the article through that date. Details of any changes may be found in the online version of the article.